09,03

Change in structure and luminescent properties of ZnSe and ZnCdSe films irradiated by electron beam

© V.A. Kravets, Ye.V. Dementyeva, A.A. Sitnikova, I.V. Sedova, M.V. Zamoryanskaya

Ioffe Institute,
St. Petersburg, Russia

E-mail: vladislav2033@yandex.ru

Received October 7, 2021
Revised October 7, 2021
Accepted October 10, 2021

Layers of ZnSe and $ZnCd_xSe$ ($x \sim 0.32-0.35$) grown on GaAs (001) substrates by molecular beam epitaxy method were investigated. The electron beam impact on changes in crystal structure of specimens under examination and on their luminescent properties was studied. Methods of cathode luminescence, transmission electron microscopy, and electron microprobe analysis were applied.

It is found that irradiation of specimens in the transmission electron microscope results in stacking faults annealing accompanied by formation of ZnO precipitates with hexagonal crystal structure. Irradiation of specimens in the cathode luminescence plant results in decreased intensity of cathode luminescence layers of ZnSe and $ZnCd_xSe$ in question due to radiation-stimulated degradation processes.

Key words: point defects, irradiation by electron beam, cathode luminescence, structural changes.

DOI: 10.21883/PSS.2022.02.52971.219

1. Introduction

ZnSe-based semiconductor lasers emitting in the blue-green spectral range are demanded in many fields of science and industry — television, lighting, optoelectronics, laser navigation systems, high-quality color printing, etc. [1].

The main problem in producing injection blue-green lasers is related to the difficulties in doping *p*-type wide-band semiconductors A^2B^6 due to thermodynamic instability of the nitrogen acceptor [2], that results in quick degradation of the laser diode and, hence, short service life of the device.

Thus, an increased focus was put on the development of alternative ways to produce laser generation which do not require $p-n$-junction and ohmic contacts, specifically on creation of A^2B^6/A^3N blue-green laser converters [3,4]) and A^2B^6 electron beam pumped semiconductor lasers (EBPSL) [5]. In recent research activities values of the electron working energy required for their operation at room temperature were decreased down to $4-10$ keV, a generation was obtained at record-low values of the electron beam threshold current density — about $0.5\,A/cm^2$ [6], and the use of laser assembly made it possible to obtain radiation pulses with a power of more than 600 W [7]. The possibility was demonstrated of EBPSL operation for several hours without decrease in output power, and it was shown that, in all likelihood, it is the quantity of faults in the initial heterostructure that is the determining factor for the service life of lasers [8]. Thus, the research of results of electron beam impact on individual layers of ZnSe and ZnCdSe, which are basic materials in laser heterostructures, is important today.

This work reports the results of investigation of the layer degradation process in ZnSe and $ZnCd_xSe$ ($x \sim 0.32-0.35$) with a layer thickness of ~ 1 mkm under irradiation by electron beam. An estimate is made for the impact of the degradation process on the luminescent properties of the material.

2. Specimens and methods of study

Layers of ZnSe (№ 688) and ZnCdSe (№ 707 and № 713) with cubic structure of zinc-blende (sphalerite) type were produced by the method of molecular beam epitaxy (MBE) on GaAs (001) substrates using a buffer layer of GaAs in the double-chamber MBE setup (SemiTeq, Russia). The films were examined using methods of local cathode luminescence (CL), transmission electron microscopy (TEM), and electron microprobe analysis (EMA).

Structural perfection of the specimens was studied by TEM method in the cross-section geometry in the bright field mode using JEM-2100F (Jeol) and EM 420 (Philips) electron microscopes. Specimens were prepared in the geometry of cross section. The specimens were thinned through etching by Ar^+ ions. Then, the study of specimens was composed of 3 stages.

1. Using the TEM method, in the cross-section geometry images of initial specimens were recorded at low currents ($I = 1$ nA) of the electron beam. The beam mode was selected in such a way as to avoid visible changes in properties of the layer under examination.

2. Then previously examined areas were additionally irradiated in TEM by electron beam (with a beam current of $I = 25-100$ nA), which resulted in specimen degradation

Table 1. Results of film studies by EMA, CL and TEM methods

Specimen	Thicknesses layers, nm	Concentration of observed defects of stacking, cm^{-2}	Film composition, obtained by method of PCMA	Position peak edge band (300 K), eV	Position band peak, associated with point defects (300 K), eV
№ 688	870	$< 1 \cdot 10^7$	ZnSe	2.7	–
№ 713	890	$\sim 2 \cdot 10^8$	$Zn_{0.68}Cd_{0.32}Se$	2.29	1.78 1.91
№ 707	600	$\sim 4 \cdot 10^8$	$Zn_{0.65}Cd_{0.35}Se$	2.26	1.77

processes visible to the operator (emergence of inclusions, change in quantity of stacking faults).

Specimens № 688 and 713 were irradiated in the JEM-2100F (Jeol) microscope with the following parameters of the electron beam: current — 100 nA, energy — 100 keV, beam radius — 1 mkm. Specimen № 707 was irradiated in the EM 420 (Philips) microscope with the following irradiation mode: energy of electrons — 200 keV, current — 25 nA, beam radius — 1 mkm.

3. Then TEM-images were recorded for the irradiated areas at low currents of the electron beam ($I = 1$ nA).

Cathode luminescence studies and electron microprobe analysis of specimens were carried out using CAMEBAX electron microprobe analyzer by Cameca equipped with four X-ray spectrometers and optical spectrometers of original design [9]. This device allows recording of CL spectra and measuring composition of the material in an area of ~ 1 mkm.

CL-studies of specimen properties were conducted at both room temperature (300 K) and liquid nitrogen temperature (77 K), with the following characteristics of electron beam: energy of electrons — 10 keV, electron beam current — 100 nA, electron beam radius — 2 mkm. CL-spectra of the irradiated area were recorded at 4–5 min intervals with a total specimen irradiation time of 20 min, while spectrum recording time was 2 min.

Composition of both the initial specimens and the specimens irradiated by electron beam was measured by EMA method with an electron energy of 10 keV, a specimen current of 15 nA, and an electron beam radius of 2 mkm. ZnSe and CdSe films were used as references. The depth of electron beam penetration for ZnSe/GaAs and ZnCdSe/GaAs structures at an electron energy of 10 keV was not greater than thickness of the films under examination.

3. Experimental results and discussion

3.1. Study of the initial films

Fig. 1 shows CL-spectra of specimens № 688, 713 and 707 recorded at room temperature within the first two minutes of electron beam irradiation. It should be noted that there were no any significant changes in CL-spectra observed within this interval of time.

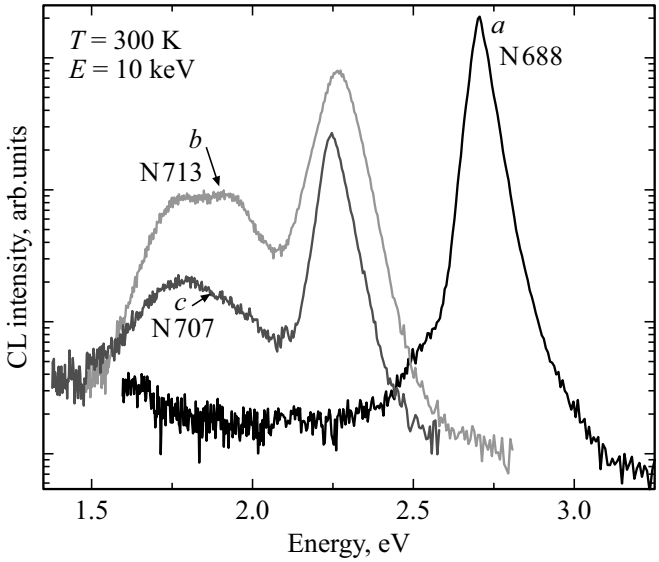

Figure 1. Spectra of CL-specimens recorded within the first two minutes of irradiation by electron beam in semi-log scale: *a*) ZnSe № 688, *b*) ZnCdSe № 713 and *c*) ZnCdSe № 707.

In the CL-spectra (Fig. 1) bands of intrinsic edge luminescence of films are observed (hereinafter referred to as „edge bands“) with peaks in the region of 2.7 eV (№ 688), 2.29 eV (№ 713) and 2.26 eV (№ 707). Along with these bands, in specimens № 713 and 707 bands related to luminescence of point defects are observed (hereinafter referred to as „wide bands“) in the range from 1.5 to 2 eV. The position of peak of this band in the CL-spectrum of specimen № 707 was observed in the region of 1.83 eV. Specimen № 713 had a wide band in the form of doublet with two peaks at 1.78 and 1.91 eV, which is considerably different from the spectrum of specimen № 707. In literature these bands are associated with complexes of point defects with involvement of vacancies [10], which corresponds to the transition of donor — double-charge vacancy of zinc (D-V_{Zn-2}), which is described in [11].

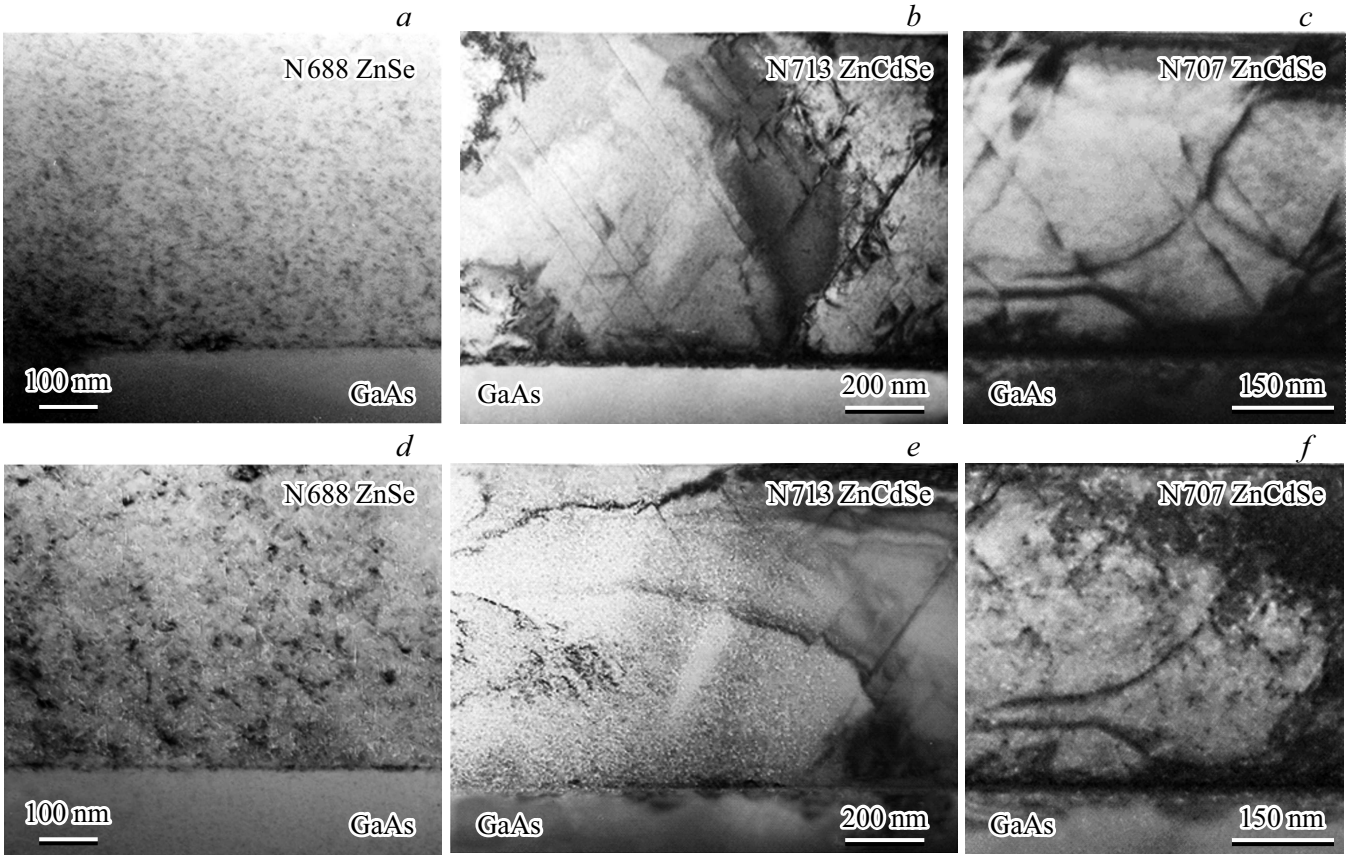

Figure 2. TEM-images before irradiation of specimens: *a*) — № 688, *b*) — № 713, *c*) — № 707; TEM-images of specimens after irradiation by electron beam: *d*) — № 688, *e*) — № 713, *f*) — № 707. The images were recorded with an electron beam energy of 100 keV for specimens № 688 and № 713 and 200 keV for specimen № 707, current density in both cases was about $I \sim 1$ nA.

Fig. 2, *a, b*, shows bright field images of initial specimens recorded by TEM method in the geometry of cross-section. These images were used to estimate concentrations of observed stacking faults and determine thickness of the films under examination. Results of these studies are presented in Table 1.

TEM-image of specimen № 688 is shown in Fig. 2, *a*. Concentration of observed stacking faults is less than $1 \cdot 10^7$ cm^{-2}. At the same time an array of dark inclusions is observed with a contrast typical for small precipitates, which do not affect the pattern of electron diffraction in Fig. 3, *a*. In the microdiffraction pattern there are clearly visible diffraction reflections corresponding only to ZnSe compound.

In the image in cross section geometry of specimens № 713 and 707 there are clearly visible stacking faults (Fig. 2, *b, c*), incipient at the ZnSe/GaAs heterovalent interface. Concentration of observed staking faults is $\sim 2 \cdot 10^8$ and $\sim 4 \cdot 10^8$ cm^{-2}, respectively. Composition of ZnCdSe layers was determined by EMA method in randomly selected 5–10 points. The studies have shown that the films are homogenous in terms of their composition.

3.2. Irradiation by electron beam with an energy of 100 and 200 keV

Fig. 2 shows bright field TEM-images recorded in the same range for the specimens before irradiation by electron beam (Fig. 2, *a, b, c*) and after irradiation (Fig. 2, *d, e*) by electron beam with an energy of 100 keV (№ 688, 713) and 200 keV (№ 707).

After irradiation of specimen № 688 the TEM-image shows large inclusions (Fig. 2, *d*) than those visible before the irradiation (Fig. 2, *a*). Comparing the images of initial (Fig. 2, *b, c*) and irradiated (Fig. 2, *e, f*) specimens № 713 and 707, it can be seen that after the irradiation the contrast associated with stacking faults disappears and dark inclusions — precipitates — appear. According to the microdiffraction data, the precipitates emerging in all specimens after irradiation, are ZnO hexagonal inclusions (Fig. 3, *b*).

Also, after the irradiation bright inclusions have emerged in all specimens with a contrast typical for pores.

Thus, the irradiation of specimens in the conditions of high power density of the electron beam with energies of 100 and 200 keV resulted in reduced number of stacking faults in the epitaxial layers. At the same time, this process

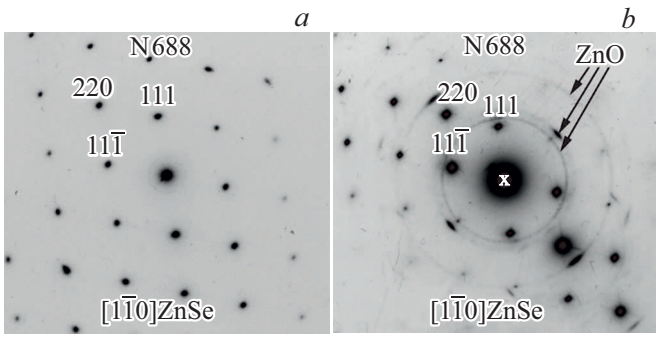

Figure 3. *a*) microdiffraction of specimen № 688 area before the irradiation in TEM, *b*) microdiffraction of the irradiated area of specimen № 688.

is accompanied by formation of pores and hexagonal precipitates of zinc oxide in the layers under examination.

3.3. Irradiation by electron beam with an energy of 10 kev

Fig. 4 shows CL-spectra of all specimens recorded during irradiation at high currents of the electron beam: $I = 100$ nA. In the process of irradiation at room temperature CL intensity has decreased significantly in all specimens. Also, it's worth to note that in the process of irradiation the composition of specimens remained unchanged at the determination accuracy of $\pm 1\%$ rel., i. e. no evaporation of Se was observed.

The reduced CL intensity may be related to both the process of film degradation and the growth of contamination hydrocarbon film similar to that examined in [12]. The method of atomic force microscopy was used to measure thickness of the contamination film formed on the specimen after 20 min of electron beam irradiation. Mean thickness of the film was ~ 50 nm. According to [13], a film of this thickness has radiation absorption strength $\sim 30\%$ of the intensity at 2.7 eV, $\sim 20\%$ at 2.25 eV, and $\sim 10\%$ at 1.84 eV. In our case it means that absorption in the range of edge bands is not more than 30% of total intensity, and the absorption the range of wide bands is not more than 10%. Therefore, it can be assumed that the observed decrease in CL intensity is related not only with the contamination film formation.

As can be seen in Fig. 4, a significant change in the shape of the wide band is observed under irradiation of the specimen № 713 at room temperature. In the process of electron beam irradiation, in the CL-spectrum of specimen № 713 the doublet with two peaks is transformed into one wide band with a peak of 1.85 eV (Fig. 5). For specimen № 713 reflection spectra were recorded, which were further recalculated to absorption spectra (Fig. 5). In the spectrum, interference oscillations typical for $Zn_{0.68}Cd_{0.32}Se$ film with a thickness of 1 mkm were observed. It can be seen in Fig. 5 that the peak of the wide band of specimen № 713 in the CL spectrum and

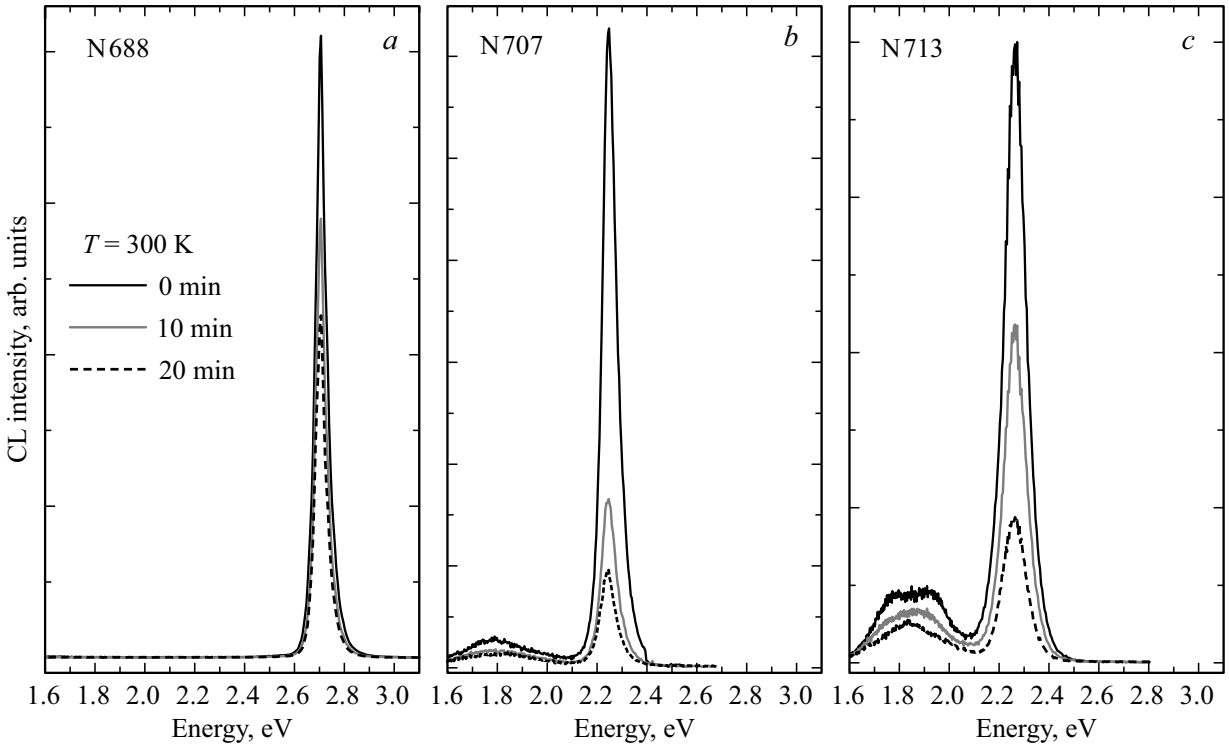

Figure 4. CL-spectra recorded in the process of electron beam irradiation of specimens *a*) ZnSe № 688, *b*) ZnCdSe № 707 and *c*) ZnCdSe № 713 at a temperature of $T = 300$ K. Time of the specimen irradiation (0, 10, 20 min) is specified in the figure.

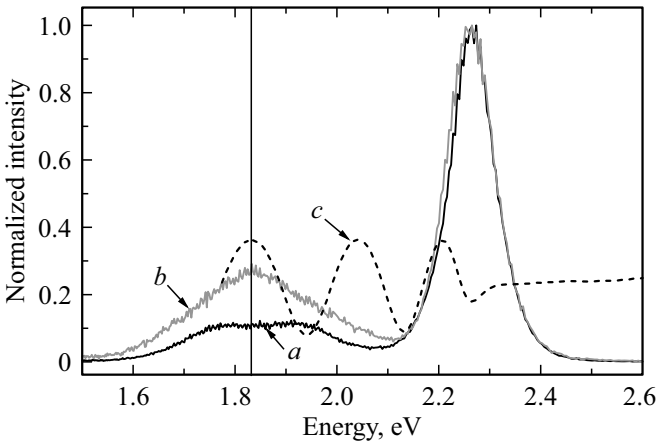

Figure 5. *a*) CL--spectrum of specimen № 713 without pre-irradiation, *b*) CL--spectrum of specimen № 713 after 20 min of irradiation and *c*) absorption spectrum of specimen № 713.

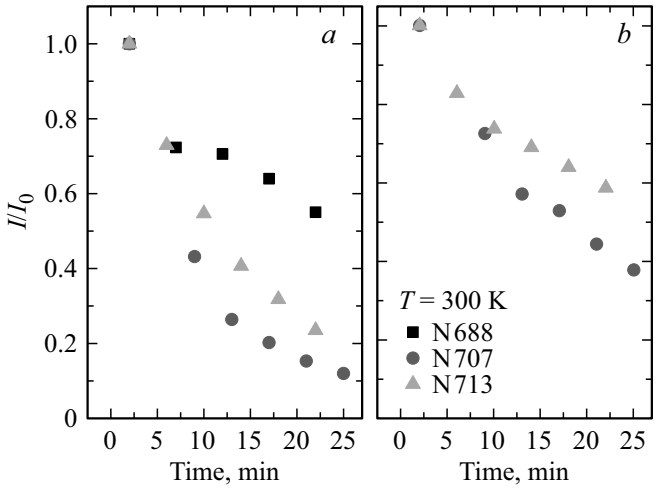

Figure 6. Intensities of CL bands as functions of electron beam irradiation times at a temperature of $T = 300$ K. *a*) change in the intensity of edge band luminescence, *b*) change in the intensity of wide band luminescence. Number of the specimen is specified in the figure.

one of absorption peaks in the region of 1.85 eV coincide with each other. Therefore, the change in shape of the wide band in spectra is probably related to the leveling out of the interference absorption as a result of electron beam irradiation.

In Fig. 6 the intensities of CL bands are shown as functions of electron beam irradiation times.

Fig. 6, *a* demonstrates that in CL studies within 20 min of irradiation by electron beam the intensity of edge bands radiation decreases by more than 50% for all specimens. CL intensity of wide bands (Fig. 6, *b*) decreases slower than the intensity of edge bands. To determine the nature of the wide band CL intensity decrease process, the change in their CL intensity depending on time (decay time) was measured before and after irradiation by electron beam (Table 2).

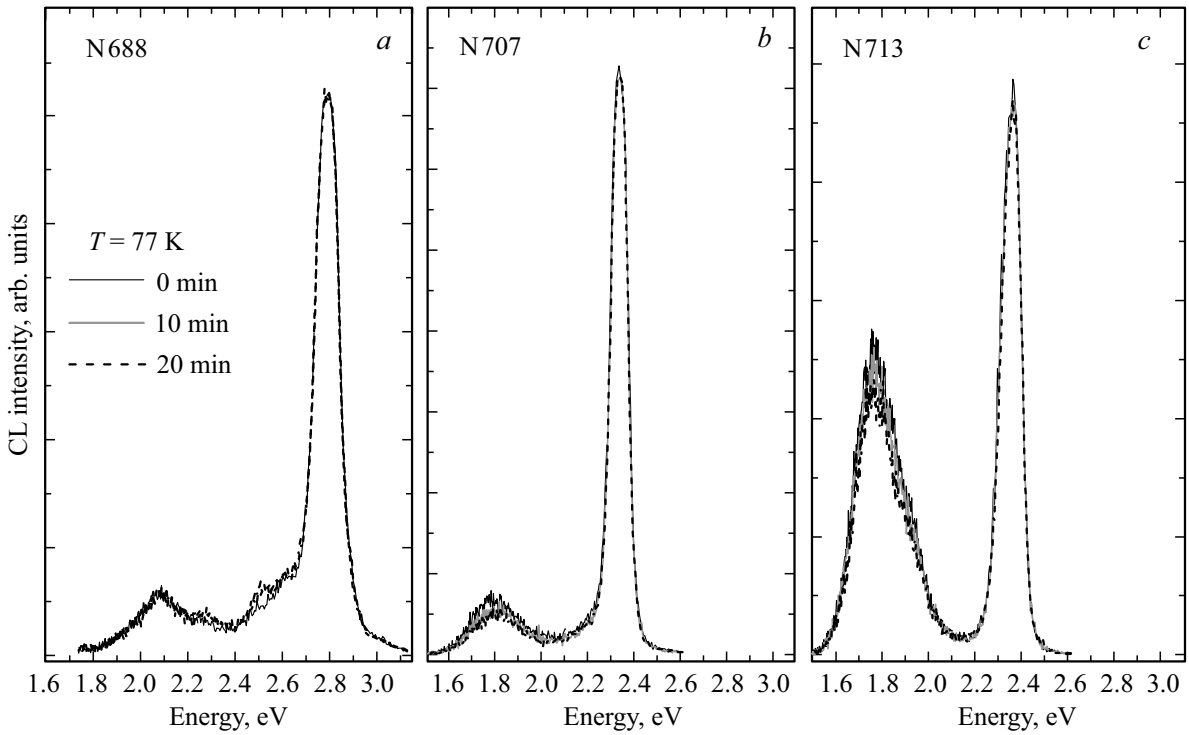

Figure 7. CL-spectra recorded in the process of electron beam irradiation of specimens *a*) ZnSe № 688, *b*) ZnCdSe № 713 and *c*) ZnCdSe № 707 at a temperature of 77 K. Time of specimen irradiation before the start of recording of the corresponding spectrum is specified in the figure.

Table 2. Decay time of wide bands before and after irradiation by electron beam

Specimen		Decay time of wide band,mks
№ 713	before irradiation	3.6
	after irradiation	4.1
№ 707	before irradiation	3.3
	after irradiation	4.3

To determine the impact of temperature on the processes of defects formation, the electron beam irradiation was conducted with simultaneous recording of CL spectra also at a temperature of 77 K, as shown in Fig. 7. In CL spectra of all specimen recorded at 77 K, a temperature shift of the edge band by 0.8 eV relative to the band position at $T = 300$ K was observed, which was related to the known effect in semiconductors — an increase in energy-gap width at specimen cooling, which is consistent with literature data [16]. The ratio of wide band intensity to edge band intensity at 77 K increased in all specimens. Also, at 77 K a wide band in the spectrum of specimen № 688 is manifested. The irradiation was conducted at the same parameters of electron beam as in the experiment at room temperature. At the same time, it should be noted that shape and intensity of CL spectra of all specimens remained unchanged at the irradiation for 20 min. Absence of changes in the spectra at a temperature of 77 K can be explained by the fact that probability of defects formation as a result of the irradiation decreases with decrease in temperature [17].

4. Discussion of results. Processes in specimens under the impact of electron beam

The degradation of the specimen irradiated by electron beam can take place due to radiation-stimulated processes or as a result of local heating of the specimen due to electron braking in the material [1]. These two degradation mechanisms are worth to be considered separately.

4.1. Local heating of the specimen by electron beam

To compare the local radiation heating during the investigations using TEM and CL methods, the heating of irradiated microvolume of ZnSe was estimated theoretically. The estimate was made for the maximum used current of the electron beam during irradiation. When calculating the temperature of heating, it was assumed that 100% of the electron beam energy lost in the specimen is converted into heat. This assumption makes it possible to calculate maximum possible temperature of the local radiation heating.

With irradiation in the CL-setup (the length of electron penetration into the specimen is less than thickness of the specimen under examination), the shape of heat generation area was approximated by a semi-ellipsoid (Fig. 8, *a*), where semiaxes were the radius of electron beam *b* and the depth of penetration of electron beam into the specimen in several places — *a*. The depth of electron beam penetration was modelled in Casino v.2.4.8.1 software package. With an electron beam accelerating voltage of 10 keV, the depth of penetration into ZnSe is ~ 400 nm.

According to [18], the maximum temperature of heating of the specimen microvolume when generating heat in an oblate ellipsoid of rotation ($a < b$) can be estimated by the following formula

$$T_{\max} = \frac{q_0(a,b)}{2k} \frac{ab^2}{\sqrt{(b^2-a^2)}} \operatorname{arct}\left(\frac{a}{\sqrt{(b^2-a^2)}}\right),$$

where $q_0(a,b)$ — energy lost in unit volume of the specimen and k — thermal conductivity coefficient of ZnSe, b — radius of electron beam, a — depth of electron beam penetration into the specimen.

With irradiation in the TEM (the length of electron penetration into the specimen is considerably greater than thickness of the layer under examination) the shape of heat generation area was approximated by a cylinder (Fig. 8, *b*) with a radius equal to that of the electron beam *b*. Height of the cylinder was taken equal to mean thickness of the thinned specimen *a* (100 nm). The portion of the energy lost in the ZnSe layer with a thickness of 100 nm was modelled in the Casino v.2.4.8.1 software package.

In this case the temperature of specimen microvolume heating is calculated by the following formula [19]:

$$T_{\max} = \frac{q_0(a,b)}{4k} b^2,$$

where $q_0(a,b)$ — energy lost in unit volume of the specimen and k — thermal conductivity coefficient of ZnSe, b — radius of electron beam.

Results of heating temperature calculation and conditions of the irradiation are given in Table 3.

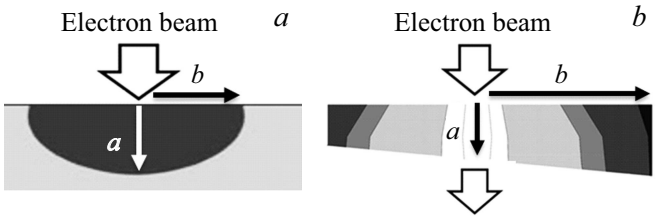

Figure 8. The area of electron beam interaction with the bulk specimen in a CL (*a*) setup and with the thinned specimen in a TEM-setup (*b*). Where *a* — depth of electron beam penetration into the specimen, *b* — radius of the electron beam.

Table 3. The calculated temperature of ZnSe heating at various irradiation modes

Method of investigation	CL	TEM	TEM
Electron beam energy E, keV	10	100	200
Specimen current I, nA	100	100	25
Electron beam energy$b$, mkm	2	1	1
Depth of penetration of electron beam into the specimen a, nm	400	100	100
$T_{\max}$, K	5	26	5

In the case of ZnCdSe triple compound with cubic structure, it is difficult to calculate theoretically the heating temperature, because there are no values of thermal conductivity in literature for this compound. It is known from literature, that due to disorder of the system, thermal conductivity of $A_xB_{1-x}C$ three-component compounds as a rule is several times less than the thermal conductivity of AC or BC two-component compounds [20]. Thus, the heating of ZnCdSe films can be several times bigger than that of ZnSe at the same conditions of the irradiation. Accordingly, the temperature of ZnCdSe heating must be more than 200°C during irradiation in the TEM setup and more than 50°C during irradiation in the CL setup. This heating is not enough to change structure of the material, because compounds based on ZnSe and ZnCdSe possess thermal stability at temperatures up to 400−600°C [21,22].

Thus, the local heating of specimens by electron beam can not explain all the effects observed in this work.

4.2. Radiation impact at elastic and nonelastic interaction of electron beam with specimen

Let us consider the issue of radiation damages at elastic scattering of electrons on atoms of the material. Formation of radiation defects — Frenkel pairs in an ideal crystal lattice under impact of an electron beam as a rule has a threshold nature. The energy of Frenkel pair formation in a ZnSe crystal is 7.6 eV for the cation sublattice (Zn) and 8.2 eV for the anion sublattice (Se) [1]. Maximum energy that can be transferred from an electron to atom of the substance at elastic scattering is defined by the following formula:

$$E_{\max} = \frac{2E^1(E^1 + 2m_0c^2)}{Mc^2}, \qquad (1)$$

where E^1 — energy of the primary electron beam, m_0 — electron mass, M — mass of the atom on which the electron is scattered, c — speed of light.

The electron energy calculated by formula (1), which is necessary to shift a Zn atom into an interstice must exceed 190 keV, and the electron energy to shift a Se atom into an interstice must exceed 240 keV. It is worth to note that the presence of defects in the crystal may result in decrease in the energy of radiation defects formation.

Since cadmium has sufficiently large atomic weight, its participation in the process of defect formation under elastic interaction of the electron beam with the specimen can be neglected.

With nonelastic interaction of the electron beam with the specimen, radiation damages of semiconductor material arise due to ionization of the atom by electrons [23]. At the moment of atom ionization the probability of this atom shift from its site to an interstice under the action of thermal oscillations increases significantly due to weakening of exchange couplings and decreased potential barrier. In [23] it is said that radiation disturbances in semiconductor materials due to ionization of atoms may take place under exposure to an electron beam with an energy of a few keV or more.

Thus, in the case of irradiation by electron beam in the TEM-setup at an energy of 200 keV, radiation damages will be observed being related to both elastic and nonelastic scattering of the electron beam on atoms of the specimen, and in the case of irradiation by electron beam in the CL-setup at an energy of 10 keV, the most likely prevailing will be the radiation damages observed at nonelastic interaction of the electron beam with the semiconductor material.

5. Discussion of results of electron beam irradiation with an energy of 100 and 200 kev in the TEM-setup

The irradiation results in formation of radiation defects in the cation sublattice (Zn). The consequence of this is the formation of pores and precipitates of ZnO in the irradiated material.

The formation of pores is most probably takes place due to zinc vacancies migration and clustering [1]. The formation of hexagonal precipitates of ZnO takes place as a result of interaction of the interstice zinc with oxygen. The presence of oxygen in specimens is probably related to the process of sample preparation (the specimens are thinned by ion etching in the air).

The processes taking place under irradiation by electron beam with an energy of 100 keV are not qualitatively different from those with an energy of 200 keV. Although the energy of 100 keV is not sufficient to form radiation defects in the crystal lattice of ZnSe under elastic interaction of the electron beam with the specimen, this fact can be explained be the existence of defects formed in the process of growth. This results in distortion of crystal lattice and decrease in the energy required to form radiation defects, which makes the irradiation energy of 100 keV also sufficient to form the observed structural changes.

6. Discussion of results of electron beam irradiation with an energy of 10 kev in the CL-setup

The change in cathode luminescence characteristics (decrease in the intensity of cathode luminescence, increase in decay times of wide bands) takes place under irradiation by electron beam with an energy of 10 keV at room temperature only. Absence of changes in the spectra at a temperature of 77 K can be explained by the fact that probability of radiation defects formation decreases with decrease in temperature. Thus, the probability of atoms shift from a lattice site into an interstice in the material under impact of thermal oscillations depends directly on the temperature [12].

The observed decrease in the intensity of edge luminescence at room temperature (Fig. 6, *a*) can be related to the emergence of point defects or their conglomerates, that act as centers of radiationless recombination [14]. This is confirmed by the fact that the most quick intensity drop is observed in the specimens with initially large number of stacking faults affecting the speed of defect formation when the specimen is irradiated by the electron beam.

The intensity of wide bands associated with zinc vacancies drops slower than the intensity of edge bands (Fig. 6, *b*). The decrease in intensity of these bands can be explained by both the decrease in concentration of luminescence centers and the formation of additional centers of radiationless recombination. To determine the nature of this process, decay times of radiation wide bands were measured before and after the irradiation by electron beam (Table 2). The increase in decay time as a result of electron beam irradiation gives evidence of decrease in the number of intrinsic defects that are centers of luminescence. Using the procedure described in [11], the change in concentrations of these centers of luminescence was calculated. The relationship for the content of centers of luminescence can be defined as follows:

$$\frac{N_1}{N_2} = \frac{I_{1\tau_1^{-1}}}{I_{2\tau_2^{-1}}},$$

where N — content of luminescent centers, I — intensity of luminescence, τ — decay time of the correspondent band.

The calculation has shown that the concentration of radiating centers after irradiation decreases significantly: in specimen № 707 — by 2.6 times, in specimen № 713 — by 1.7 times. The decrease in concentration of luminescence centers gives evidence of radiation-stimulated annealing or transformation of luminescent centers into defects, which results in decrease in intensity of wide band luminescence. A similar calculation was performed for specimen № 688, because this specimen had no wide band observed at room temperature. Perhaps the electron beam irradiation leads to formation of conglomerates of zinc vacancies, which results in change in their energy position within the band and, hence, to decrease in concentration of luminescent centers.

Thus, the decrease in intensity of edge luminescence band takes place due to the emergence of radiationless recombination centers. And the decrease in intensity of wide bands can be explained by the decrease in concentration (transformation or annealing) of luminescence centers.

7. Conclusion

With the irradiation of specimens in the transmission electron microscope annealing of stacking faults was observed together with formation of ZnO precipitates with hexagonal crystal structure and emergence of pores. The formation of ZnO precipitates and pores is related to the extensive formation of zinc vacancies. No selenium evaporation or clustering was observed. It is shown that processes taking place under irradiation by electron beam with an energy of 100 keV are not qualitatively different from those with an energy of 200 keV.

When investigating the impact of irradiation on the luminescent properties of structures, it was shown that the processes of CL intensity decrease are only observed at room temperature and are irreversible. The decrease in CL intensity of bands in spectra is resulted from radiation-stimulated processes of defect formation. The decrease in intensity of edge luminescence band takes place due to the formation of radiationless recombination centers and the increase in the portion of radiationless transitions. The decrease in wide band intensity is related to the decrease in content of luminescence centers associated with zinc vacancies. Perhaps the process of transformation or annealing of luminescent centers is observed.

Funding

The TEM studies were performed using the equipment of the federal Common Research Center „Materials Science and Diagnostics in Advanced Technologies“, supported by the Ministry of Education and Science of Russia (Unique project identifier: RFMEFI62119X0021).

Conflict of interest

The authors declare that they have no conflict of interest.

References

[1] Yu.Yu. Loginov, Paul D. Brown, Ken Dyurouz, Regularities of formation of structural defects in semiconductors A^2B^6. Logos, M. (2003). 304 p. (in Russian).

[2] S. Gundel, D. Albert, J. Nurnberger, W. Faschinger. Phys. Rev. B **60**, R16271 (1999).

[3] S.V. Sorokin, I.V. Sedova, S.V. Gronin, G.V. Klimko, K.G. Belyaev, S.V. Ivanov, A. Alyamani, E.V. Lutsenko, A.G. Vainilovich, G.P. Yablonskii. Electron. Lett. **48**, *2*, 118 (2012).

[4] A.G. Vainilovich, E.V. Lutsenko, V.N. Pavlovskii, G.P. Yablonskii, A. Alyamani, M. Aljohenii, A. Aljerwii, S.V. Gronin, S.V. Sorokin, I.V. Sedova, S.V. Ivanov. Phys. Status Solidi B **253**, *8*, 1498(2016).
[5] M.M. Zverev, S.V. Sorokin, N.A. Gamov, E.V. Zhdanova, V.B. Studionov, I.V. Sedova, S.V. Gronin, S.V. Ivanov. Phys. Status Solidi C **13**, *7–9*, 661 (2016).
[6] M.M. Zverev, N.A. Gamov, Ye.V. Zhdanova, D.V. Peregudov, V.B. Studenov, S.V. Ivanov, I.V. Sedova, S.V. Sorokin, S.V. Gronin, P.S. Kop'yev, Letters to the Journal of Technical Physics **33**, *24*, 1 (2007) (in Russian).
[7] M.M. Zverev, N.A. Gamov, E.V. Zdanova, V.N. Studionov, D.V. Peregoudov, S.V. Sorokin, I.V. Sedova, S.V. Gronin, P.S. Kop'ev, I.M. Olikhov, S.V. Ivanov. Phys. Status Solidi B **247**, *6*, 1561 (2010).
[8] M.M. Zverev, N.A. Gamov, Ye.V. Zhdanova, D.V. Peregudov, V.B. Studenov, S.V. Gronin, I.V. Sedova, S.V. Sorokin, S.V. Ivanov, Surface, **5**, 1 (27) (in Russian).
[9] M.V. Zamoryanskaya, S.G. Konnikov, A.N. Zamoryanskii Instrum. Exp. Tech. **4**, 477 (2004).
[10] L.V. Borkovska, N.O. Korsunska, V.I. Kushnirenco. Semicond. Phys. **6**, *3*, 294 (2003).
[11] K.M. Lee, D. Le Si, G.D. Watkins. Solid State Commun. **35**, *7*, 527(1980).
[12] K.N. Orekhova, Yu.M. Serov, P.A. Dement'ev, Ye.V. Ivanova, V.A. Kravets, V.P. Usacheva, M.V. Zamoryanskaya, Journal of Technical Physics **89**, *9*, 1412 (2009) (in Russian).
[13] A.Yu. Mester, A.N. Trofimov, M.V. Zamoryanskaya, A.M. D'yakonov. Tech. Phys. **59**, *10*, 1536 (2014).
[14] H. Casey, M. Panish, Heterostructure Lasers Mir, M. (1981). V. 2. 358 p. (in Russian)
[15] Ye.V. Ivanova, M.V. Zamoryanskaya, Physics of the Solid State, **58**, 1895 (2016) (in Russian).
[16] A.A. Shakhmin, I.V. Sedova, S.V. Sorokin, H.-J. Fitting, M.V. Zamoryanskaya. Physica B: Condens. Matter **404**, *23–24*, 5016 (2009).
[17] B.I. Boltax, Diffusion and point defects in semiconductors. Nauka, L. 1972), 384 p. (in Russian).
[18] L.A. Bakaleynikov, Ye.V. Galaktionov, V.V. Tretyakov, E.A. Tropp, Physics of the Solid State **43**, *5*, 779 (2001) (in Russian).
[19] M.V. Zamoryanskaya, Ye.V. Ivanova, A.A. Sitnikova, Physics of the Solid State **53**, *7*, 1399 (2011) (in Russian).
[20] G.N. Dul'nev, Yu.P. Zarichnyak, Thermal conductivity of mixtures and composite materials. Energiya, Leningrad, (1974), 264 p. (in Russian).
[21] T. Yokogawa, P.D. Floyd, J.L. Merz, H. Luo, J.K. Furdyna. J. Cryst. Growth **138**, 564 (1994).
[22] T. Yokogawa, J.L. Merz, H. Luo, J.K. Furdyna, S. Lau, M. Kuttler, D. Bimberg. Jpn. J. Appl. Phys. **34**, 1159 (1995).
[23] V.S. Vavilov, A.Ye. Kiv, O.R. Niyazova, Mechanisms of formation and migration of defects in semiconductors. Nauka, M. (1981).